doi:10.1093/brain/awr204 Brain 2011: 134; 2844–2854 | 2844

BRAIN
A JOURNAL OF NEUROLOGY

Morphometric MRI analysis improves detection of focal cortical dysplasia type II

Jan Wagner,[1,2] Bernd Weber,[1,2,3] Horst Urbach,[4] Christian E. Elger[1,2,3] and Hans-Jürgen Huppertz[5]

1 Department of Epileptology, University of Bonn, D-53127 Bonn, Germany
2 Department of NeuroCognition/Imaging, Life and Brain Centre, D-53127 Bonn, Germany
3 Centre for Economics and Neuroscience, University of Bonn, Bonn, D-53127 Germany
4 Department of Radiology/Neuroradiology, University of Bonn, D-53127 Bonn, Germany
5 Swiss Epilepsy Centre, CH-8008 Zürich, Switzerland

Correspondence to: Jan Wagner, MD,
Department of Epileptology,
University of Bonn,
Sigmund-Freud-Str. 25,
D-53127 Bonn, Germany
E-mail: jan.wagner@ukb.uni-bonn.de

Focal cortical dysplasias type II (FCD II) are highly epileptogenic lesions frequently causing pharmacoresistant epilepsy. Detection of these lesions on MRI is still challenging as FCDs may be very subtle in appearance and might escape conventional visual analysis. Morphometric MRI analysis is a voxel-based post-processing method based on algorithms of the statistical parametric mapping software (SPM5). It creates three dimensional feature maps highlighting brain areas with blurred grey–white matter junction and abnormal gyration, and thereby may help to detect FCD. In this study, we evaluated the potential diagnostic value of morphometric analysis as implemented in a morphometric analysis programme, compared with conventional visual analysis by an experienced neuroradiologist in 91 patients with histologically proven FCD II operated on at the University Hospital of Bonn between 2000 and 2010 (FCD IIa, $n = 17$; IIb, $n = 74$). All preoperative MRI scans were evaluated independently (i) based on conventional visual analysis by an experienced neuroradiologist and (ii) using morphometric analysis. Both evaluators had the same clinical information (electroencephalography and semiology), but were blinded to each other's results. The detection rate of FCD using morphometric analysis was superior to conventional visual analysis in the FCD IIa subgroup (82% versus 65%), while no difference was found in the FCD IIb subgroup (92% versus 91%). However, the combination of conventional visual analysis and morphometric analysis provided complementary information and detected 89 out of all 91 FCDs (98%). The combination was significantly superior to conventional visual analysis alone in both subgroups resulting in a higher diagnostic sensitivity (94% versus 65%, $P = 0.031$ for FCD IIa; 99% versus 91%, $P = 0.016$ for FCD IIb). In conclusion, the additional application of morphometric MRI analysis increases the diagnostic sensitivity for FCD II in comparison with conventional visual analysis alone. Since detection of FCDs on MRI during the presurgical evaluation markedly improves the chance of becoming seizure free postoperatively, we apply morphometric analysis in all patients who are MRI-negative after conventional visual analysis at our centre.

Keywords: epilepsy; MRI; presurgical evaluation; image processing

Abbreviations: FLAIR = fluid-attenuated inversion recovery; CVA = conventional visual analysis; FCD = focal cortical dysplasia; MAP = morphometric analysis programme; MRI = magnetic resonance imaging

Received May 5, 2011. Revised June 9, 2011. Accepted June 11, 2011. Advance Access publication September 5, 2011

Introduction

Focal cortical dysplasias type II (FCD II), according to the classification of Palmini and Lüders, and the recent classification proposal of Blümcke and colleagues (Palmini and Luders, 2002; Palmini *et al.*, 2004; Blumcke *et al.*, 2011), are highly epileptogenic lesions often associated with medically intractable focal epilepsy (Frater *et al.*, 2000; Sisodiya, 2004; Fauser *et al.*, 2006). They are histologically well defined by the presence of dysmorphic neurons in FCD IIa and additional balloon cells in FCD IIb (Palmini and Luders, 2002; Palmini *et al.*, 2004; Blumcke *et al.*, 2011). Because of the high rate of pharmacoresistance, many patients suffering from epilepsy caused by FCD undergo presurgical evaluation. Detection of these lesions on MRI during the presurgical workup is crucial, since both the probability of undergoing surgical therapy and the postoperative outcome are significantly better in MRI-positive patients (Berg *et al.*, 2003; Bien *et al.*, 2009). However, FCDs may be very subtle on MRI and their detection is still challenging, although MRI techniques have markedly improved over recent years. Referring to FCD II, 20–30% of cases are reported to be MRI-negative by conventional visual analysis (CVA) (Tassi *et al.*, 2002; Widdess-Walsh *et al.*, 2005; Krsek *et al.*, 2008).

In order to improve the detection and delineation of FCDs, a voxel-based morphometric MRI analysis was introduced in 2005 (Huppertz *et al.*, 2005). This method is based on algorithms of the freely available statistical parametric mapping software (SPM5, Wellcome Department of Imaging Neuroscience Group; http://www.fil.ion.ucl.ac.uk/spm) and highlights brain regions with blurring of the grey–white matter junction and abnormal extension of grey matter into white matter (i.e. abnormal deep sulci). These abnormalities are typical MRI features of FCD (Barkovich and Kuzniecky, 1996; Lee *et al.*, 1998; Urbach *et al.*, 2002; Colombo *et al.*, 2003; Besson *et al.*, 2008).

Whether this method has a real benefit compared with CVA and therefore should be performed in all patients undergoing presurgical evaluation who are MRI-negative after CVA has not thus far been investigated systematically. The aim of this study was to evaluate the potential diagnostic value of morphometric MRI analysis in patients with histologically proven FCD II by comparing the detection rate using morphometric MRI analysis with that of CVA by an experienced neuroradiologist at a specialized tertiary epilepsy centre. We did not analyse FCD type I according to Palmini and Lüders in this study, because the Department of Neuropathology at the University of Bonn does not diagnose this entity (see 'Discussion' section for details).

Materials and methods

Study group

We analysed all patients with histologically proven FCD IIa or IIb who were operated on for pharmacoresistant epilepsy at the University Hospital of Bonn between 2000 and 2010. Exclusion criteria were unavailable preoperative MRI including a 3D T1 data set necessary for the MRI post-processing and gross movement artefacts or extensive brain abnormalities, which might disturb the normalization and segmentation.

MRI protocol

All patients included in the study underwent presurgical MRI examinations. Until 2005, MRI was performed using a 1.5 tesla scanner (Intera, Philips Medical Systems; $n = 45$), thereafter a 3 tesla system was utilized (Trio, Siemens or Intera, Philips Medical Systems; $n = 46$). The following sequences were acquired in each patient: a 3D T_1-weighted gradient-echo sequence (voxel size $1 \times 1 \times 1$ mm) consisting of 140–160 sagittal slices, coronal and axial fluid-attenuated inversion recovery (FLAIR) images (slice thickness 2–5 mm), coronal and axial T_2-weighted images (slice thickness 2–5 mm) and axial T_1-weighted images (slice thickness 5 mm) after injection of Gadolinium-diethylene triamine pentaacetic acid. If temporal lobe epilepsy was suspected, the axial and coronal images were acquired with a modified angulation oriented along the hippocampus.

MRI post-processing

Morphometric MRI analysis is a voxel-based image processing method comparing individual brain anatomy with a normal database. The technique applies algorithms of SPM5 and additional simple computations and is described in detail elsewhere (Huppertz *et al.*, 2005; Wellmer *et al.*, 2010). Briefly, a T_1-weighted MRI volume data set is normalized to Montreal Neurological Institute space while simultaneously correcting for intensity inhomogeneities, and segmented in different tissue compartments for grey matter, white matter and the rest using the 'unified segmentation' algorithm of SPM5 with its default settings (warping regularization = 1; warp frequency cut-off = 25; bias regularization = 0.0001; bias full width at half maximum = 60; voxel size = $1 \times 1 \times 1$ mm). The distribution of grey and white matter is analysed on a voxel-wise basis and compared with a normal database. This database, which has been described elsewhere (Huppertz *et al.*, 2008), consists of 150 controls (70 female, mean age at MRI 30.9 years, range 15–77 years) with MRIs acquired on five different MRI scanners and found to be free of structural abnormalities. Based on this analysis, 3D feature maps, called 'extension image' and 'junction image', are created. These are *z*-score maps in which brain structures that deviate from the normal database have higher *z*-scores and appear bright, thereby highlighting typical MRI features of FCDs, such as abnormal gyration and abnormal extension of grey matter into white matter (extension image) and blurring of the grey–white matter junction (junction image). Currently, there is no use of thresholds or SPM statistics for automated lesion detection. The whole processing is performed by a fully automated MATLAB script called Morphometric Analysis Programme (MAP). By highlighting suspicious cortical regions, the MAP results can guide a second look at the MRI and thereby increase the sensitivity of MRI evaluation.

MRI evaluation

All MRI scans were evaluated prospectively by an experienced neuroradiologist (H.U.) for possible epileptogenic lesions during the presurgical workup. Clinical data (EEG and semiology) were provided if available. MRI criteria suggestive of FCD were as follows: (i) focal thickening of the cortex; (ii) blurring of the grey–white matter junction; and (iii) hyperintense signal of the cortex and/or the subcortical white matter on T2 and/or FLAIR. If H.U. described the MRI either as normal or exhibiting abnormalities that were not considered epileptogenic, the patient was classified as CVA-negative (CVA^-). If H.U.

diagnosed FCD or (in rare cases) other abnormalities that were considered epileptogenic (which histologically turned out to be FCD as well), the patient was classified as CVA-positive (CVA^+).

MRI post-processing was performed by J.W., a neurologist who had the same clinical data as H.U., but no information about the results of the CVA. This was done retrospectively for the MRI data before 2006 and prospectively for MRI data thereafter. The morphometric maps were evaluated in the following manner: if a clear and focal abnormality could be detected in at least one of the two feature maps, the co-registered structural MRI was visually inspected at this location for signs suggestive of FCD. If the structural scan was also considered to be abnormal at this location, the patient was classified as MAP-positive (MAP^+). It has to be noted that this analysis using MAP is also a visual evaluation and does not make use of any automated detection algorithm. Instead, the visual evaluation is augmented by feature maps, which can be regarded as new MR sequences used in addition to the conventional structural MR images.

Postoperative outcome

Postoperative outcome was determined according to Engel's classification (Engel *et al.*, 1993). We classified seizure freedom strictly as Engel Ia (seizure free, no auras). However, to allow a comparison with other studies, which define seizure freedom as Engel Ia to Id, we also report this category (referred to as Engel I_{total}).

Statistical analyses

Statistical analyses were performed using SPSS 18.0 for Windows (SPSS Inc.). For statistical comparisons of independent ordinal data, a Fisher's exact test was performed; for comparisons of paired ordinal data, a McNemar test; and for comparisons of independent metrical data, a Mann–Whitney U Test. $P \leqslant 0.05$ was regarded as statistically significant. Diagnostic yield was defined as the rate of cases detected by one method and not by the other.

Results

Study group

Between 2000 and 2010, 1059 patients underwent resective surgery for pharmacoresistant epilepsy at the University Hospital Bonn. Among these, 102 patients (10%) had the histopathological diagnosis of FCD II. Seven patients had no preoperative MRI including a 3D T1 scan necessary for the post-processing, and four patients were excluded because of gross movement artefacts. Ninety-one patients were subsequently included in the study, 17 had the histological diagnosis of FCD IIa and 74 additionally showed balloon cells in the histological specimen (FCD IIb). In two patients (one with FCD IIa and one with FCD IIb), the FCD was associated with ipsilateral hippocampal sclerosis. Since hippocampal sclerosis affects neither the post-processing itself nor the interpretation of the feature maps, both patients were included. Clinical data of the study group are summarized in Table 1. There were no significant differences concerning the age distribution between FCD type IIa and IIb, and between patients measured at 1.5 and 3 tesla, respectively.

FCDs were preferentially located in the frontal lobe ($n = 51$), followed by temporal and parietal (both $n = 12$), occipital ($n = 5$) and insular ($n = 4$) locations. In the remaining seven cases, more than one lobe was involved.

CVA versus MAP

Taking FCD IIa and IIb together, 82 out of the 91 FCDs (90%) were detected using MAP. The detection rate was better in FCD IIb compared with FCD IIa (92% versus 82%); this difference was not statistically significant ($P = 0.361$).

When comparing the impact of the two different feature maps, the junction image was superior to the extension image in both groups (71% versus 41%, $P = 0.180$ for FCD IIa; 91% versus 70%, $P < 0.001$ for FCD IIb). However, in three cases (two with FCD IIa, one with FCD IIb) only the extension image revealed the FCD. Results are summarized in Fig. 1A.

In all, 78 out of all 91 FCDs were CVA^+ (86%). CVA detected FCD IIb significantly better than FCD IIa (91% versus 65%, $P = 0.014$). When comparing CVA with MAP, a higher detection rate using MAP could be observed in the cases with FCD IIa (82% versus 65%, $P = 0.453$). No difference between CVA and MAP was found in the FCD IIb group (91% versus 92%; Fig. 1B). Among the six CVA^- patients with FCD IIa diagnosed by CVA, MAP helped to detect the dysplasia in five of them (diagnostic

Table 1 Clinical and postoperative outcome data of the study group

	All	FCD IIa	FCD IIb	1.5 tesla	3 tesla
n (male)	91 (46)	17 (9)	74 (37)	45 (22)	46 (24)
Median age at epilepsy onset, years (range)	5.0 (0.1–41.0)	6.0 (0.1–41.0)	4.0 (0.1–32.0)	3.0 (0.1–25.0)	6.0 (0.1–41.0)
Median age at surgery, years (range)	23.6 (2.1–58.3)	19.7 (4.9–56.0)	29.5 (2.1–58.3)	23.6 (2.1–58.3)	24.2 (4.9–57.9)
Median age at MRI, years (range)	23.2 (2.1–58.3)	19.3 (2.5–55.9)	29.3 (2.1–58.3)	23.2 (2.1–58.3)	23.9 (2.5–57.9)
Patients aged <18 years at MRI, *n* (%)	28 (31)	6 (35)	22 (30)	14 (31)	14 (30)
Patients aged <30 months at MRI, *n* (%)	2 (2)	0 (0)	2 (3)	2 (4)	0 (0)
Outcome					
Median follow-up, years (range)	2.7 (1.0–10.8)	2.3 (1.1–8.0)	2.8 (1.0–10.8)	5.2 (1.0–10.8)	2.0 (1.0–3.7)
Engel Ia, *n* (%)	65 (71)	10 (59)	55 (74)	29 (64)	36 (78)
Engel I_{total}, *n* (%)	70 (77)	11 (65)	59 (80)	32 (71)	38 (83)
Engel II, *n* (%)	3 (3)	2 (12)	1 (1)	2 (4)	1 (2)
Engel III, *n* (%)	16 (18)	4 (23)	12 (16)	11 (24)	5 (11)
Engel IV, *n* (%)	2 (2)	0 (0)	2 (3)	0 (0)	2 (4)

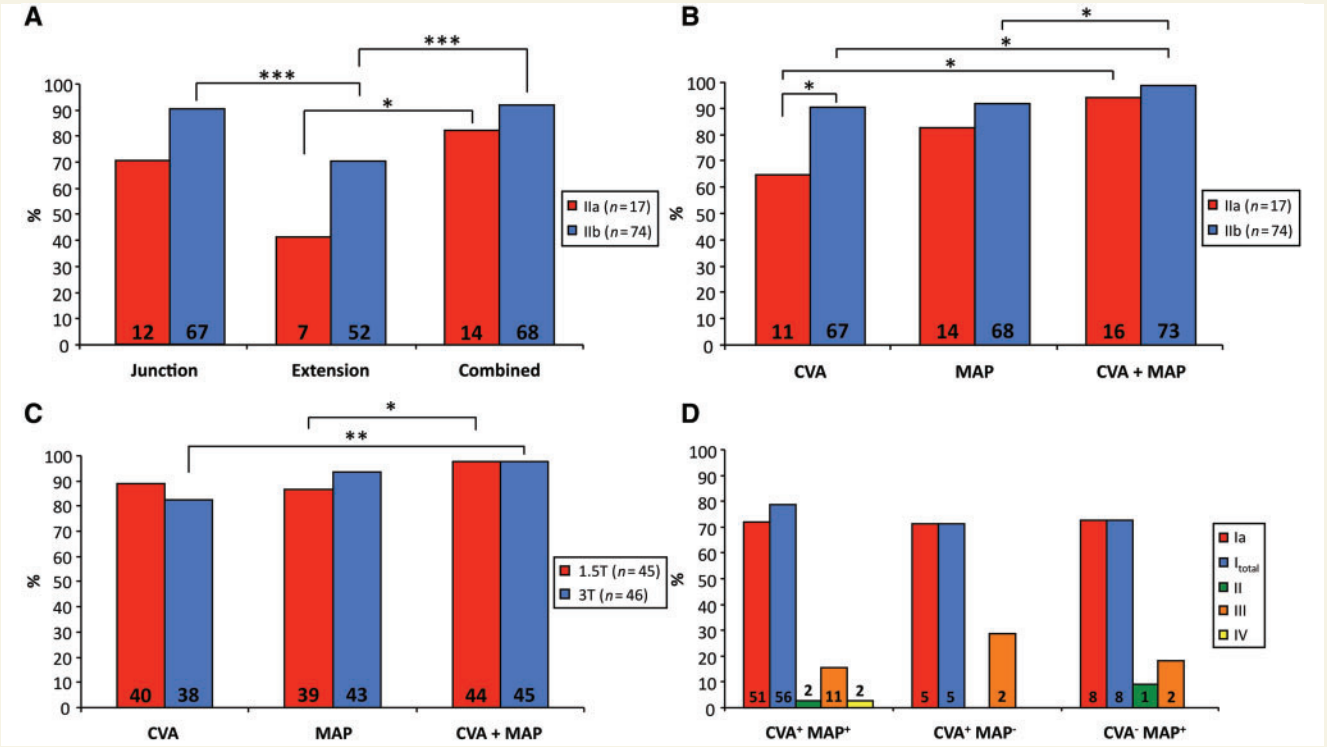

Figure 1 (**A**) Detection rate of the two feature maps and the combination of both maps for FCD IIa and IIb. (**B**) Detection rate of CVA, MAP and the combination of both methods for the two FCD types. (**C**) Detection rate in relation to MRI field strength. (**D**) Postoperative outcome in relation to results of CVA and MAP (see text for details). Numbers within the bars represent numbers of patients investigated in each group. Ia, I_{total}, II, III, IV = outcome class according to Engel's classification; $*P \leqslant 0.05$; $**P \leqslant 0.01$; $***P \leqslant 0.001$.

yield of 29% in relation to a total of 17 cases with FCD IIa). Vice versa, two out of the three MAP^- patients with FCD IIa were CVA^+, so that only one patient with FCD IIa remained negative after evaluation using both methods. Results are summarized in Fig. 1B and examples of some FCD IIa cases that were either only MAP^+ or CVA^+ are shown in Fig. 2.

In the group with FCD IIb, six out of seven CVA^- lesions could be detected by using MAP (diagnostic yield 8%; examples in Fig. 3) and CVA was positive in five out of six MAP^- patients (examples in Fig. 4). Thus, with the combination of these two approaches, 89 out of all 91 cases with FCDs (98%) could be detected. This was significantly superior to CVA alone in both groups (94% versus 65%, $P = 0.031$ for FCD IIa; 99% versus 91%, $P = 0.016$ for FCD IIb). In comparison with MAP alone, a significant difference was only found in the group with FCD IIb (99% versus 92%, $P = 0.031$). Two patients included in the study were aged <30 months at the time of MRI. The FCDs in these two cases were detected in both approaches, i.e. CVA and MAP.

Effect of field strength

The FCD detection rate with the help of MAP was higher in patients undergoing 3 tesla MRI compared with 1.5 tesla (94% versus 87%, $P = 0.315$), while we found opposite results for CVA (83% versus 89 %, $P = 0.551$). Furthermore, the diagnostic yield of MAP was higher in patients undergoing 3 tesla MRI compared with 1.5 tesla (15% versus 11%). The additional application of MAP led to a significantly higher detection rate in the 3 tesla group in comparison with CVA alone (98% versus 83%, $P = 0.008$), while no significant difference was found in the 1.5 tesla group (98% versus 89%, $P = 0.063$). Referring to the 1.5 tesla patients, the combination of CVA and MAP was significantly superior to MAP alone (98% versus 87%, $P = 0.031$). Results are illustrated in Fig. 1C.

Postoperative outcome

Taking all 91 patients together, 71% became completely seizure free postoperatively (Engel Ia). An additional 6% achieved an Engel I outcome other than Ia (= 77% Engel I_{total}). Only 2% had no improvement in seizure frequency after the operation. The postoperative seizure freedom rate was higher in the group with FCD IIb compared with the group with FCD IIa, although this difference was not statistically significant ($P = 0.169$). Postoperative outcome data are summarized in Table 1.

Correlating the results of CVA and MAP with the postoperative outcome, we found no significant differences between those who had concordant CVA and MAP results and those who were either only MAP^+ or CVA^+. Results are illustrated in Fig. 1D.

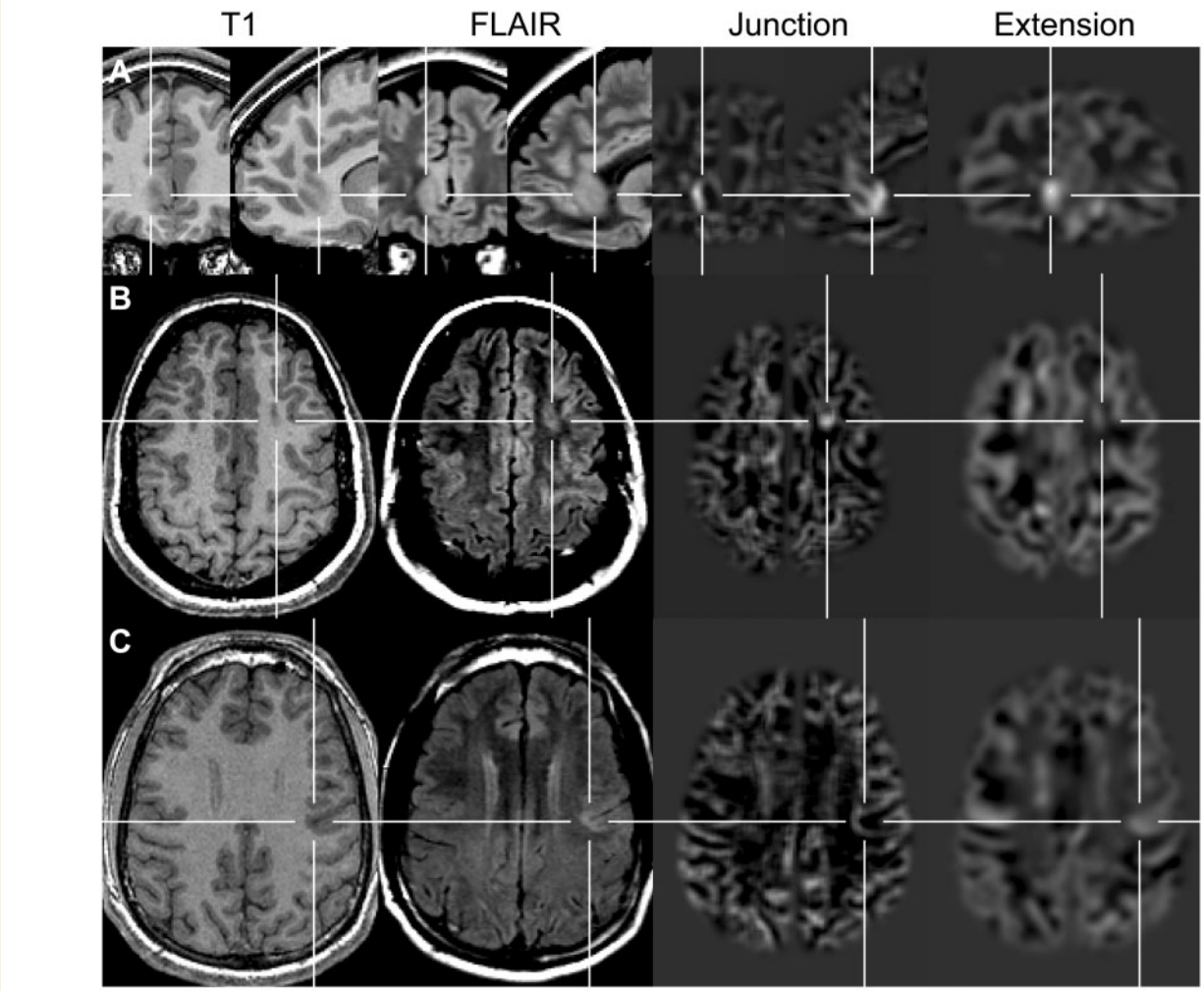

Figure 2 Examples of three FCD IIa lesions that were either only MAP$^+$ (**A** and **B**) or only CVA$^+$ (**C**). The junction image highlights brain areas with a blurred grey–white matter junction and the extension image emphasizes grey matter extending abnormally into the white matter (abnormally deep sulci). Corresponding areas are shown on co-registered T1 and FLAIR images. (**A**) Right frontomesial FCD that escaped CVA, but was clearly visible on both feature maps. (**B**) CVA$^-$ FCD IIa located at the bottom of the left superior frontal sulcus with a moderate abnormality visible in the junction image, while no abnormality was visible in the extension image. (**C**) MAP$^-$ FCD IIa located at the bottom of the left inferior frontal sulcus. No clear abnormality could be detected in the feature maps, while a discrete thickening and hyperintensity of the cortex was visible especially on the axial FLAIR images.

Discussion

FCD II is an increasingly recognized cause of pharmacoresistant epilepsy, accounting for 10% of all patients undergoing epilepsy surgery at our centre. However, detection on MRI in many cases is still challenging as FCDs may be very subtle and might remain unrecognized after CVA (Woermann and Vollmar, 2009). Detection of these lesions, especially during presurgical evaluation, is crucial as it significantly improves the chance of becoming seizure-free postoperatively (Bien *et al.*, 2009). In this study, we evaluated the potential diagnostic value of a voxel-based morphometric MRI analysis tool called MAP by comparing the detection of FCDs using this tool with CVA by an experienced neuroradiologist. Main findings of this study are discussed in the following.

Feature maps

The detection rate by help of the 'junction' image was superior to the 'extension' image for both FCD IIa and IIb, supporting the findings of the previous study reporting on this post-processing method (Huppertz *et al.*, 2005). These results are most likely explained by the fact that blurring of the grey–white matter junction is more frequently associated with FCD II than abnormal sulcal patterns (Krsek *et al.*, 2008, 2009). However, in three cases only the extension image revealed the FCD, demonstrating the importance of both feature maps.

CVA versus MAP

Although being a specialized tertiary epilepsy centre putting great efforts in MRI diagnostics, 14% of all FCD II remained

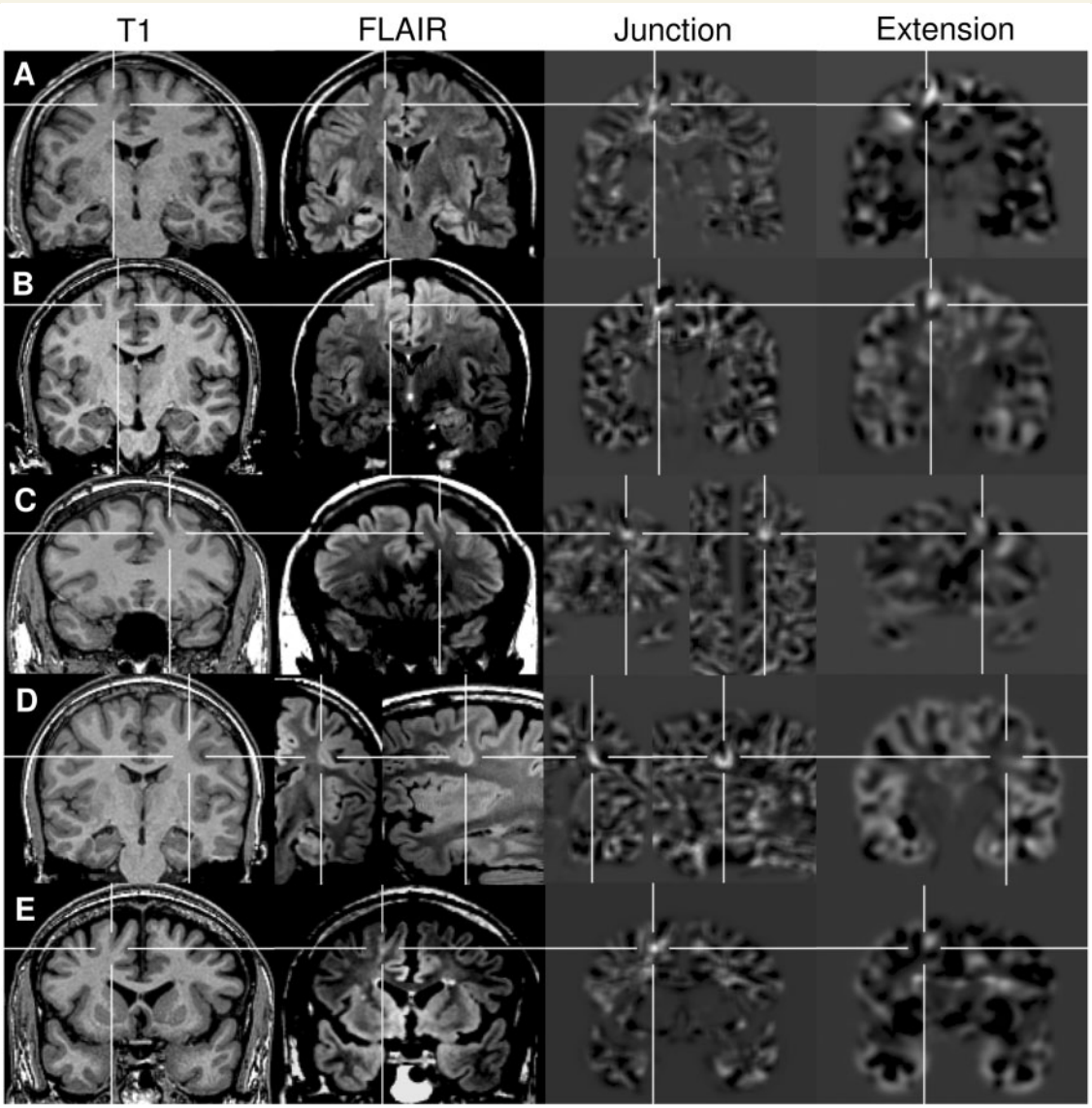

Figure 3 Five CVA$^-$ FCD IIb lesions that could be detected by MAP. The junction image was positive in all illustrated cases, while the extension image showed a clear abnormality only in the first two examples (**A** and **B**).

undetected by CVA. FCD IIa lesions remained significantly more often unrecognized by CVA in comparison with FCD IIb. This is in accordance with other studies reporting about MRI features of FCD II and most likely caused by the fact that FCD IIa lesions often appear more discretely on MRI due to the lack of a marked hyperintense subcortical zone (Widdess-Walsh *et al.*, 2005, 2006; Krsek *et al.*, 2008; Colombo *et al.*, 2009; Blumcke *et al.*, 2011). In this subgroup, five of six CVA$^-$ FCD IIa lesions could be detected with the help of MAP, leading to a diagnostic yield of 29%.

Referring to the subgroup with FCD IIb, there was no difference in the detection rate between CVA and MAP. The detection rate of both methods alone was >90% in each case, which is superior to most previous reports (Widdess-Walsh *et al.*, 2005; Krsek *et al.*, 2008). However, the combination of CVA and MAP provided complementary information and led to a significant improvement of the detection rate in comparison with each method in isolation (diagnostic yield of 7–8%).

In summary, the additional application of MAP led to a higher detection rate in both FCD subgroups, resulting in an increased diagnostic sensitivity. Taking FCD IIa and IIb together, 89 out of all 91 cases could be detected after evaluation using both methods. This very high detection rate reflects the outstanding role of MRI evaluation at our centre. We now apply MAP routinely in all patients who are negative after CVA. Furthermore, the application of MAP is not limited to FCDs alone. It can also detect subtle forms of subcortical band heterotopia, which might escape CVA (Huppertz *et al.*, 2008).

Effect of field strength

The FCD detection rate and the diagnostic yield of MAP were higher using 3 tesla MRI data for post-processing compared

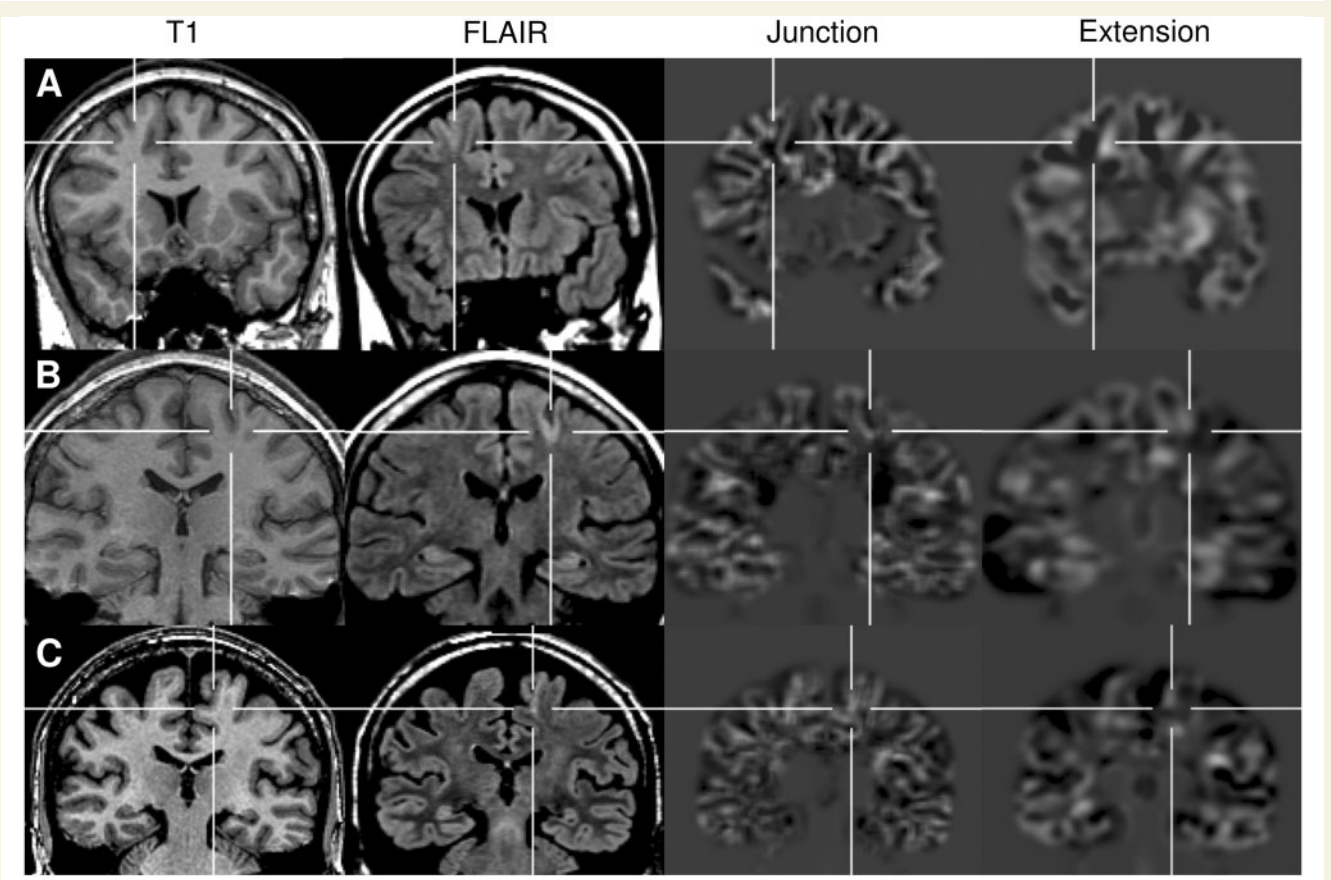

Figure 4 Three examples of CVA$^+$ but MAP$^-$ FCD IIb lesions. Although very subtle abnormalities (especially thickening of the cortex and subcortical hyperintensity) could be detected by CVA, both feature maps showed no clear abnormality in these patients.

with 1.5 tesla. We suspect that the higher contrast-to-noise ratios of 3 tesla MRI improve the segmentation results, i.e. the basis for morphometric analysis, and thereby promote the results of post-processing more than those of CVA. The benefit of 3 tesla compared with 1.5 tesla in MRI post-processing has not yet been investigated. Some publications indicate that previously unrecognized lesions on 1.5 tesla can be revealed by CVA at higher field strengths (Knake *et al.*, 2005; Strandberg *et al.*, 2008; Bernasconi *et al.*, 2011). However, in the cited studies, all patients underwent both low-field and high-field MRI and the detection of epileptogenic lesions on these scans was compared. In our study, all subjects underwent either 1.5 tesla or 3 tesla MRI and therefore our results cannot be compared directly with the previous studies.

Postoperative outcome

The postoperative seizure outcome in our study group was similar to previous reports about epilepsy surgery in FCD II (Tassi *et al.*, 2002; Colombo *et al.*, 2003; Krsek *et al.*, 2008). We found no significant differences in the postoperative outcome between those patients who had concordant CVA and MAP results and those who were either only MAP$^+$ or CVA$^+$. Eleven CVA$^-$ patients benefitted from MAP since their FCD was detected by this approach and the postoperative outcome in these patients was superior to seizure freedom rates in MRI-negative cases reported in the literature (Bien *et al.*, 2009). Furthermore, patients with concordant semiological and EEG findings in whom a lesion can be detected on MRI may be operated on without prior invasive recordings. In contrast, invasive diagnostics are necessary in most MRI-negative cases, increasing the risk of postoperative neurological deficits.

Comparison with other MRI post-processing studies

Huppertz *et al*. (2005) investigated the application of MAP in 25 patients with histologically proven FCD I and II according to Palmini and Lüders (2002). In their study, MAP provided additional information to CVA in four patients (diagnostic yield 16%), which is comparable with the results of our study. However, the false negative rate of 16% was slightly higher compared with our results (10%), which might be explained by the ongoing improvements of MRI techniques and growing experience in application and evaluation of this post-processing method. In a preliminary study with MRI post-processing based on the extension image only (Kassubek *et al.*, 2002), FCDs were detected in six of seven patients investigated, but only one was histologically confirmed and all lesions were previously known.

Bastos *et al*. (1999) applied curvilinear reformatting in five patients with FCD, all of them being negative after CVA. All five patients could be detected using curvilinear reformatting, but the study group was too small to make a substantial conclusion concerning the diagnostic yield. Furthermore, no FLAIR images were acquired, decreasing the diagnostic sensitivity of CVA and no histological subtypes of the four operated patients were provided.

In the study by Bernasconi *et al*. (2001), the diagnostic value of a voxel-based post-processing method creating maps that highlight cortical thickening, blurring of the grey–white matter junction and relative signal intensity was evaluated. Sixteen patients with histologically proven FCD were studied; eight out of these were negative by CVA. Application of MRI post-processing detected additional six FCDs resulting in a significant increase of the sensitivity (diagnostic yield 38%). Similar to the study of Bastos *et al*. (1999), the study group was relatively small and no differentiation between the FCD subtypes was provided.

The same method was applied in a series of 23 patients with histologically proven FCDs of the subtypes Ib, IIa and IIb (Colliot *et al.*, 2006*a*). In all 23 patients, the dysplasias could be detected by MRI post-processing, including seven who were negative by initial CVA of the clinical MRI, resulting in a diagnostic yield of 30%.

A similar approach, i.e. the calculation of FCD-specific feature maps as the ratio of cortical thickness and local intensity gradient, but combined with automated lesion detection by statistical parametric mapping, was used by Srivastava *et al*. (2005) in 17 patients with FCD and 64 controls. The method correctly located the lesion in 9 of 17 cases (53%), using a threshold that minimized false positives and 12 of 17 cases (71%), using a threshold that allowed more false positive results. The method could also identify two lesions which previously had only been detected by help of Subtraction Ictal SPECT Co-registered to MRI (SISCOM; diagnostic yield 12%).

Three studies reported on the application of voxel-based morphometry in the detection of FCD (Bonilha *et al.*, 2006; Colliot *et al.*, 2006*b*; Bruggemann *et al.*, 2009). However, all patients investigated in these studies were CVA^+, so that no conclusion about the diagnostic benefit of the post-processing can be drawn.

The use of a surface-based technique in patients with cortical malformations was evaluated in a recently published study by Thesen *et al*. (2011). The authors reported high values for sensitivity and specificity of their method, but only five patients with FCD were included in the study and all were CVA^+, so that again no conclusions about the diagnostic benefit can be drawn.

In contrast to all of the studies cited above, in which the post-processing was based on T1 data sets, the following two studies used FLAIR images for the analysis. Riney *et al*. (2011) applied voxel-based morphometry of FLAIR images in eight patients with CVA^+ FCDs and 14 patients with cryptogenic epilepsy. The post-processing detected seven out of eight CVA^+ FCDs and two additional suspected cases among the cryptogenic patients, resulting in a diagnostic yield of 20% (i.e. two out of a total of 10 patients with FCD could additionally be detected by the post-processing).

Focke *et al*. (2008) introduced another voxel-based FLAIR analysis and applied it to 25 cases with FCD. Twenty-two cases could be detected by their technique, but all cases were CVA^+. Main findings of the cited studies are summarized in Table 2.

In summary, our study provides by far the largest group of patients with FCD in whom the diagnostic value of MRI post-processing has been investigated and the results are in line with the studies of Bernasconi *et al*. (2011) and Colliot *et al*. (2006*a*) which also demonstrate a significant benefit of MRI post-processing in comparison with CVA alone.

Apart from MRI post-processing, there are other techniques that can be co-registered with MRI and may help in identifying cortical dysplasia. PET, magnetoencephalography and single-photon emission CT have been reported to have comparable sensitivity in detecting FCD in comparison with MAP (Bast *et al.*, 2004; Dupont *et al.*, 2006; Knake *et al.*, 2006; Madan and Grant, 2009; Chassoux *et al.*, 2010). However, in contrast to these techniques MAP does not incur additional costs and is no additional burden on the patient as it can be performed using conventional MRI data that is acquired routinely during the pre-surgical evaluation.

Limitations

The design of this study (i.e. inclusion of patients only) did not allow evaluation of the specificity of both methods. Neither for CVA nor for MAP was it documented and assessed whether there were false-positive findings. In addition, if a subtle lesion in a patient with epilepsy suspected either by CVA or MAP does not become resected, it is principally not possible to confirm that this is not a true lesion. However, until now there has been no case of FCD suspected by MAP, which after resection in our clinic turned out not to be FCD according to histology. Above all, it is also clear that the epileptogenicity of a suspected lesion is not determined by MRI investigation but must be confirmed by EEG findings.

As there was only one investigator for each branch of this study (i.e. CVA and MAP), it was not possible to calculate the interrater reproducibility of the results. The CVA was done prospectively over 10 years by the neuroradiologist with the most experience in the MRI of patients with epilepsy at this site. It would not have been possible to find another neuroradiologist at the centre with a comparable level of experience. In addition, the amount of MRI data prohibited a fully retrospective evaluation by a second or third investigator.

The morphometric analysis does not account for signal hyperintensities on FLAIR and/or T_2 images, which are often associated with FCD II. It only highlights structural abnormalities on T_1 images. As a consequence, MAP does not detect FCDs that have no structural abnormalities and are only characterized by cortical and/or subcortical hyperintensities. This fact might explain that MAP produced false-negative results in nine out of a total of 91 patients (10%); seven of these could be detected by CVA. Thus, the morphometric analysis cannot replace an experienced neuroradiologist nor obviate the need to read other MRI sequences apart from the T_1 image. MAP should be regarded as a supportive method, increasing the diagnostic sensitivity for certain lesions.

Furthermore, the interpretation of the feature maps requires an experienced reader who is familiar with the method and the resulting feature maps. It should be noted that MAP does not detect

Table 2 Publications on MRI post-processing in FCD, in chronological order

Study	*n*	FCD type	Histologically confirmed	PP method	CVA$^+$	PP$^+$	CVA + PP	Diagnostic yield	Significance
Bastos *et al.* (1999)	5	NA	4/5	Curvilinear reformatting	0/5	5/5	5/5	5/5	NA
Bernasconi *et al.* (2001)	16	NA	16/16	Voxel-based texture analysis	8/16	14/16	NA	6/16	$P < 0.003$
Kassubek *et al.* (2002)	7	NA	1	MAP (extension image only)	7/7	6/7	7/7	none	NA
Srivastava *et al.* (2005)	17	IIa, IIb	4/17	Feature-based statistical analysis	11/17	9/17	13/17	2/17	NA
Huppertz *et al.* (2005)	25	Ia, Ib, IIa, IIb	25/25	MAP	21/25	21/25	25/25	4/25	NA
Colliot *et al.* (2006*a*)	23	Ib, IIa, IIb	23/23	Voxel-based texture analysis	16/23	23/23	23/23	7/23	$P = 0.016$
Colliot *et al.* (2006*b*)	27	NA	18/27	Voxel-based morphometry	27/27	21/27	27/27	none	NA
Bonilha *et al.* (2006)	11	IIa, IIb	8/11	Voxel-based morphometry	11/11	10/11	11/11	none	NA
Focke *et al.* (2008)	25	IIb	4/25	Voxel-based FLAIR analysis	25/25	22/25	25/25	none	NA
Bruggemann *et al.* (2009)	8	NA	0/8	Voxel-based morphometry	8/8	5/8	8/8	none	NA
Thesen *et al.* (2011)	5	NA	3/5	Surface-based analysis	5/5	4/5	5/5	none	NA
Riney *et al.* (2011)	10	NA	NA	Voxel-based morphometry FLAIR	8/10	9/10	10/10	2/10	NA
Present study	91	IIa, IIb	91/91	MAP	78/91	82/91	89/91	11/91	$P < 0.001$

NA = not available; diagnostic yield = rate of FCDs detected by MRI post-processing but not by CVA; PP = post-processing.

the lesion automatically. The feature maps direct the attention of the reader to suspicious regions and can increase the conspicuity of a lesion. A visual confirmation taking into account the conventional structural scans is necessary. MAP may highlight regions that have no pathological correlate on the conventional MRI sequences, for example, regions of delayed white matter myelination in children. As explained in the 'Materials and methods' section, these regions were not regarded as MAP$^+$. It should also be mentioned that due to ongoing myelination or reversed T_1 contrasts, segmentation may fail below the age of 2 years.

Unfortunately, the analysis of FCD I according to Palmini and Lüders (2002) was not possible in this study. As a local particularity, this FCD subtype is principally not diagnosed by the Department of Neuropathology at the University of Bonn. Especially temporal pole abnormalities (i.e. white matter changes, blurring of the grey–white matter junction) associated with hippocampal sclerosis, which in other epilepsy centres are frequently addressed as FCD I, are regarded as unspecific changes or signs of delayed white matter maturation at our centre. As a consequence, the results of this study cannot be applied to FCD I. However, as mentioned above, most of the previous studies reporting on MRI post-processing in FCD did not specify the subtypes investigated.

Due to the long period of time from which the patients with FCD were included in this study (i.e. 2000–10), we had to handle MRI data acquired using different MRI scanners. Therefore, an already existing and previously described normal database with MRI data integrated from five different MR scanners of 1.5 and 3 tesla has been employed for the morphometric analysis. In our experience, the theoretical disadvantage of not using a scanner-specific normal database is compensated by the fact that a combined database is often larger and thus a better model for the variability in the normal population than a scanner-specific normal database constructed from MRI data of only a few healthy controls. However, if sufficient MRI data for controls measured using the same scanner is available, a scanner-specific normal database is still advisable.

Conclusion

In this study on all patients with FCD II operated on for pharmacoresistant epilepsy at the University Hospital of Bonn between 2000 and 2010, we could show that morphometric MRI analysis—applied in addition to CVA—significantly increases the diagnostic sensitivity for this kind of lesion. This is especially remarkable as the post-processing was applied by a non-radiologist, while the conventional visual reading of the MRI was done by an experienced neuroradiologist who has been involved in the pre-surgical evaluation of patients with epilepsy for many years. It can be assumed that the diagnostic yield of the MRI post-processing is even higher when compared with a 'normal' radiologist reading these images. As a consequence, at our centre morphometric MRI analysis is now applied in all patients with epilepsy who are MRI-negative according to CVA.

Acknowledgements

The authors are grateful to Prof. Dr Jörg Wellmer, Ruhr-University, Bochum, Germany, for introducing the morphometric MRI analysis at the Department of Epileptology in Bonn. Furthermore, we thank Nicole Klein, Department of Neuroradiology, University of Bonn, Germany, for her assistance in obtaining the MRI scans.

Funding

The study was partly supported by the SFB TR3 projects A1 and A8 of the DFG. The development of the post-processing techniques was supported by the Swiss Epilepsy Foundation and the Swiss National Science Foundation (Project No. 127581).

References

Barkovich AJ, Kuzniecky RI. Neuroimaging of focal malformations of cortical development [Review]. J Clin Neurophysiol 1996; 13: 481–94.

Bast T, Oezkan O, Rona S, Stippich C, Seitz A, Rupp A, et al. EEG and MEG source analysis of single and averaged interictal spikes reveals intrinsic epileptogenicity in focal cortical dysplasia. Epilepsia 2004; 45: 621–31.

Bastos AC, Comeau RM, Andermann F, Melanson D, Cendes F, Dubeau F, et al. Diagnosis of subtle focal dysplastic lesions: curvilinear reformatting from three-dimensional magnetic resonance imaging. Ann Neurol 1999; 46: 88–94.

Berg AT, Vickrey BG, Langfitt JT, Sperling MR, Walczak TS, Shinnar S, et al. The multicenter study of epilepsy surgery: recruitment and selection for surgery. Epilepsia 2003; 44: 1425–33.

Bernasconi A, Antel SB, Collins DL, Bernasconi N, Olivier A, Dubeau F, et al. Texture analysis and morphological processing of magnetic resonance imaging assist detection of focal cortical dysplasia in extra-temporal partial epilepsy. Ann Neurol 2001; 49: 770–5.

Bernasconi A, Bernasconi N, Bernhardt BC, Schrader D. Advances in MRI for 'cryptogenic' epilepsies. Nat Rev Neurol 2011; 7: 99–108.

Besson P, Andermann F, Dubeau F, Bernasconi A. Small focal cortical dysplasia lesions are located at the bottom of a deep sulcus. Brain 2008; 131: 3246–55.

Bien CG, Szinay M, Wagner J, Clusmann H, Becker AJ, Urbach H. Characteristics and surgical outcomes of patients with refractory magnetic resonance imaging-negative epilepsies. Arch Neurol 2009; 66: 1491–9.

Blumcke I, Thom M, Aronica E, Armstrong DD, Vinters HV, Palmini A, et al. The clinicopathologic spectrum of focal cortical dysplasias: a consensus classification proposed by an ad hoc Task Force of the ILAE Diagnostic Methods Commission(1). Epilepsia 2011; 52: 158–74.

Bonilha L, Montenegro MA, Rorden C, Castellano G, Guerreiro MM, Cendes F, et al. Voxel-based morphometry reveals excess gray matter concentration in patients with focal cortical dysplasia. Epilepsia 2006; 47: 908–15.

Bruggemann JM, Wilke M, Som SS, Bye AM, Bleasel A, Lawson JA. Voxel-based morphometry in the detection of dysplasia and neoplasia in childhood epilepsy: limitations of grey matter analysis. J Clin Neurosci 2009; 16: 780–5.

Chassoux F, Rodrigo S, Semah F, Beuvon F, Landre E, Devaux B, et al. FDG-PET improves surgical outcome in negative MRI Taylor-type focal cortical dysplasias. Neurology 2010; 75: 2168–75.

Colliot O, Antel SB, Naessens VB, Bernasconi N, Bernasconi A. In vivo profiling of focal cortical dysplasia on high-resolution MRI with computational models. Epilepsia 2006a; 47: 134–42.

Colliot O, Bernasconi N, Khalili N, Antel SB, Naessens V, Bernasconi A. Individual voxel-based analysis of gray matter in focal cortical dysplasia. Neuroimage 2006b; 29: 162–71.

Colombo N, Salamon N, Raybaud C, Ozkara C, Barkovich AJ. Imaging of malformations of cortical development. Epileptic Disord 2009; 11: 194–205.

Colombo N, Tassi L, Galli C, Citterio A, Lo RG, Scialfa G, et al. Focal cortical dysplasias: MR imaging, histopathologic, and clinical correlations in surgically treated patients with epilepsy. AJNR Am J Neuroradiol 2003; 24: 724–33.

Dupont P, Van PW, Palmini A, Ambayi R, Van LJ, Goffin J, et al. Ictal perfusion patterns associated with single MRI-visible focal dysplastic lesions: implications for the noninvasive delineation of the epileptogenic zone. Epilepsia 2006; 47: 1550–7.

Engel J Jr, Van Ness PC, Rasmussen T, Ojemann LM. Outcome with respect to epileptic seizures. In: Engel J Jr, editor. Surgical treatment of the epilepsies. 2nd edn. New York: Raven Press; 1993. p. 609–21.

Fauser S, Huppertz HJ, Bast T, Strobl K, Pantazis G, Altenmueller DM, et al. Clinical characteristics in focal cortical dysplasia: a retrospective evaluation in a series of 120 patients. Brain 2006; 129: 1907–16.

Focke NK, Symms MR, Burdett JL, Duncan JS. Voxel-based analysis of whole brain FLAIR at 3T detects focal cortical dysplasia. Epilepsia 2008; 49: 786–93.

Frater JL, Prayson RA, Morris HH III, Bingaman WE. Surgical pathologic findings of extratemporal-based intractable epilepsy: a study of 133 consecutive resections. Arch Pathol Lab Med 2000; 124: 545–9.

Huppertz HJ, Grimm C, Fauser S, Kassubek J, Mader I, Hochmuth A, et al. Enhanced visualization of blurred gray-white matter junctions in focal cortical dysplasia by voxel-based 3D MRI analysis. Epilepsy Res 2005; 67: 35–50.

Huppertz HJ, Wellmer J, Staack AM, Altenmuller DM, Urbach H, Kroll J. Voxel-based 3D MRI analysis helps to detect subtle forms of subcortical band heterotopia. Epilepsia 2008; 49: 772–85.

Kassubek J, Huppertz HJ, Spreer J, Schulze-Bonhage A. Detection and localization of focal cortical dysplasia by voxel-based 3-D MRI analysis. Epilepsia 2002; 43: 596–602.

Knake S, Halgren E, Shiraishi H, Hara K, Hamer HM, Grant PE, et al. The value of multichannel MEG and EEG in the presurgical evaluation of 70 epilepsy patients. Epilepsy Res 2006; 69: 80–6.

Knake S, Triantafyllou C, Wald LL, Wiggins G, Kirk GP, Larsson PG, et al. 3T phased array MRI improves the presurgical evaluation in focal epilepsies: a prospective study. Neurology 2005; 65: 1026–31.

Krsek P, Maton B, Korman B, Pacheco-Jacome E, Jayakar P, Dunoyer C, et al. Different features of histopathological subtypes of pediatric focal cortical dysplasia. Ann Neurol 2008; 63: 758–69.

Krsek P, Pieper T, Karlmeier A, Hildebrandt M, Kolodziejczyk D, Winkler P, et al. Different presurgical characteristics and seizure outcomes in children with focal cortical dysplasia type I or II. Epilepsia 2009; 50: 125–37.

Lee BC, Schmidt RE, Hatfield GA, Bourgeois B, Park TS. MRI of focal cortical dysplasia. Neuroradiology 1998; 40: 675–83.

Madan N, Grant PE. New directions in clinical imaging of cortical dysplasias. Epilepsia 2009; 50 (Suppl 9): 9–18.

Palmini A, Luders HO. Classification issues in malformations caused by abnormalities of cortical development. Neurosurg Clin N Am 2002; 13: 1–16, vii.

Palmini A, Najm I, Avanzini G, Babb T, Guerrini R, Foldvary-Schaefer N, et al. Terminology and classification of the cortical dysplasias [Review]. Neurology 2004; 62: S2–8.

Riney CJ, Chong WK, Clark CA, Cross JH. Voxel based morphometry of FLAIR MRI in children with intractable focal epilepsy: Implications for surgical intervention. Eur J Radiol 2011, in press.

Sisodiya SM. Surgery for focal cortical dysplasia [Review]. Brain 2004; 127: 2383–4.

Srivastava S, Maes F, Vandermeulen D, Van PW, Dupont P, Suetens P. Feature-based statistical analysis of structural MR data for automatic

detection of focal cortical dysplastic lesions. Neuroimage 2005; 27: 253–66.

Strandberg M, Larsson EM, Backman S, Kallen K. Pre-surgical epilepsy evaluation using 3T MRI. Do surface coils provide additional information? Epileptic Disord 2008; 10: 83–92.

Tassi L, Colombo N, Garbelli R, Francione S, Lo RG, Mai R, et al. Focal cortical dysplasia: neuropathological subtypes, EEG, neuroimaging and surgical outcome. Brain 2002; 125: 1719–32.

Thesen T, Quinn BT, Carlson C, Devinsky O, DuBois J, McDonald CR, et al. Detection of epileptogenic cortical malformations with surface-based MRI morphometry. PLoS One 2011; 6: e16430.

Urbach H, Scheffler B, Heinrichsmeier T, von Oertzen J, Kral T, Wellmer J, et al. Focal cortical dysplasia of Taylor's balloon cell type: a clinicopathological entity with characteristic neuroimaging and histopathological features, and favorable postsurgical outcome. Epilepsia 2002; 43: 33–40.

Wellmer J, Parpaley Y, von Lehe M, Huppertz HJ. Integrating magnetic resonance imaging postprocessing results into neuronavigation for electrode implantation and resection of subtle focal cortical dysplasia in previously cryptogenic epilepsy. Neurosurgery 2010; 66: 187–94.

Widdess-Walsh P, Diehl B, Najm I. Neuroimaging of focal cortical dysplasia. J Neuroimaging 2006; 16: 185–96.

Widdess-Walsh P, Kellinghaus C, Jeha L, Kotagal P, Prayson R, Bingaman W, et al. Electro-clinical and imaging characteristics of focal cortical dysplasia: correlation with pathological subtypes. Epilepsy Res 2005; 67: 25–33.

Woermann FG, Vollmar C. Clinical MRI in children and adults with focal epilepsy: a critical review. Epilepsy Behav 2009; 15: 40–9.